

EXPERIMENTAL RESEARCH OF THE IMPACT OF SHIP'S ROLLING ON THE PERFORMANCE OF PV PANELS

Wojciech Zeńczak* 

Zbigniew Zapałowicz 

West Pomeranian University of Technology, Poland

* Corresponding author: wojciech.zenczak@zut.edu.pl (W. Zeńczak)

ABSTRACT

The aim of the International Maritime Organization (IMO) to reduce by half the amount of greenhouse gases emitted by marine ships by 2050, and its vision of the fastest total decarbonisation in the maritime shipping industry within the present century, calls for implementation with various means of decarbonisation. The IMO approaches the process of decarbonisation in two phases. Firstly, short-term, compact projects are to be considered, next, more complex, medium- and long-term solutions should be aimed at. The preferred arrangements to be applied are photovoltaic systems. Their performance depends to a high degree on the solar incidence angle. In the case of a ship swinging as a result of its course in relation to the wave and incidence direction, the incidence angle undergoes significant periodic changes with a significant effect on the power generated by the PV panels. As a result, the total amount of energy produced by the PV panels diminishes. The paper presents experimental research results obtained on the stand that allowed the investigation of PV panels in simulated marine conditions. Two characteristic positions of a PV panel's rotation axis in relation to the solar rays' incidence direction were investigated. It was proved for both variants that the rolling period and solar incidence angle affected the power generated by the PV panel.

Keywords: ship power system, PV system, ship's energy efficiency design index, ship rolling

NOMENCLATURE

A_{PV}	panel surface area (m ²)	γ	receiver azimuth angle or solar azimuth angle (deg)
B	ship's width (m)	δ	solar declination (deg)
E	energy (J) or (Wh)	τ	time (s)
G	irradiance on horizontal surface (W/m ²)	τ_c	rolling period (s)
L	ship's overall length (m)	ω	hourly angle (deg) or circular frequency of regular wave
P	power (W)	Δ	increment
T	ship's draught (m)	Θ_A	amplitude of oscillating rotational displacements relative to axis x
X_A	amplitude of oscillating displacement relative to axis x	Θ_β	incidence angle (deg)
Y_A	amplitude of oscillating displacement relative to axis y	Φ	latitude (ship's position) (deg)
Z_A	amplitude of oscillating displacement relative to axis z	Φ_A	amplitude of oscillating rotational displacements relative to axis y
α_s	solar altitude angle (deg)	Ψ_A	amplitude of oscillating rotational displacements relative to axis z
β	inclination angle of PV panel (ship's heeling angle) (deg)		
$\beta_x, \beta_y, \beta_z, \beta_r, \beta_l, \beta_p$	phase shifts of particular motions relative to the regular sinusoidal wave		

SUBSCRIPTS

<i>LT</i>	local time
<i>LST</i>	local solar time
<i>max</i>	maximal
<i>min</i>	minimal
<i>r</i>	relative
<i>s</i>	solar
<i>z</i>	zenith

INTRODUCTION

In recent years, the International Maritime Organization (IMO) has focused strongly on preventing the emission of greenhouse gases (GHG) by ships. The IMO strategy implies that emissions of GHG should be reduced by half by 2050, as compared to 2008. By the end of the century, the maritime shipping industry should be totally decarbonized. One of the subtargets of the IMO is the reduction of GHG by at least 40% as early as 2030, compared with the year 2008. In order to achieve this target, the IMO has introduced further provisions that oblige shipowners to reduce GHG emissions. Besides the Energy Efficiency Design Index (EEDI) introduced on 1 January 2013 and applying to newly built ships with tonnage above 400 GT, new provisions were introduced in June of 2021. They will come into force on 1 January 2023. All existing merchant and passenger ships, regardless of the year of production, will be subject to the requirements of the Energy Efficiency Design Index for Existing Ships (EEXI). The index is equivalent to the EEDI index in its phase 2 or 3, with some amendments.

Furthermore, new provisions will come into force in 2023. They will oblige shipowners to annually determine the Carbon Intensity Indicator (CII) for all cargo, RoPax, and cruise ships above 5000 GT of tonnage participating in international trade. The CII determines the efficiency with which a ship transports goods or passengers, given in grams of emitted CO₂ relative to the load capacity and nautical mile. Each vessel will be given an annual rating ranging from A to E, for which the rating thresholds will become increasingly stringent each year up to 2030. For ships that are rated D or E in three consecutive years, a corrective action plan will be elaborated and endorsed as part of the SEEMP (Ship Energy Efficiency Management Plan) [1].

The EEXI index is determined once and defined by design characteristics, and permits the respective certificate to be obtained. On the other hand, the CII is an operating parameter and it determines the real emission of GHG during a ship's operating time.

This situation obliges shipowners to decide in favour of vessels that are more environmentally friendly and energy-saving [2, 3]. They can achieve this aim also by switching to alternative fuels like liquid or gas biofuels, and even solid biofuels like torrefied pellets, or ammonium hydroxide, E-fuels (PtF technology) and, as a target, hydrogen. At the same time, the ship's energy system should be modified and

made more efficient, for instance by making use of waste heat or by introducing hybrid or purely electric drives [4-6]. Increasingly popular is the application of renewable energy sources (RES), mostly wind power and irradiance, as they make it possible to obtain better parameters of the required EEDI, EEXI, and CII indexes. The application of RES on seagoing vessels with power of a few or several dozen MW is not sufficient to cover the whole energy demand of the vessel, however. RES are characterised by lower energy flux density than conventional energy sources. Hence, any effort to enhance the application efficiency of RES is significant. In the case of using PV panels on the ship, which is the subject of the present paper, one such effort is the cooling of PV panels by sea water and thus increasing their efficiency, as described, among others, in papers [7-13].

However, a number of inconveniences emerge when mounting PV panels on ships, so they can prove to be less effective than similar systems onshore. Most of all, the highly changeable environmental conditions, such as strong and changing wind, high air humidity, or the effects of sea salt aerosol, impair their efficiency. The ship's swinging and changes of its heading are among the factors that most impede the operation of PV panels. Both can be prevented by the application of systems that track the sun. Still, such systems are not used in vessels because of the probability of damage, high costs, and additional energy consumption by the system.

As a result, PV panels are most often mounted in a horizontal plane with a consequent loss of some power that could otherwise be generated [14, 15].

The phenomenon of the effect of the ship's motion on the efficiency of the PV system has been the subject of a number of investigations. In particular, the loss of part of the energy that could possibly be generated from PV panels as a result of the ship's swinging has spurred a number of hybrid solutions. They comprise, besides the PV system and traditional diesel generators, also an energy storage system. Analysis of the operational stability of such a system dedicated to a big tanker is presented by Hai Lan et al. [16]. The authors assumed the course typical for the vessel in question, the rolling period of 20s, and a heeling angle of 16°. In these conditions, the irradiance changed in the range of ca 780 W/m² to 1000 W/m², with frequency relative to the rolling period. Simulation research of the proposed flywheel kinetic energy storage showed high efficiency in power stabilisation of the whole energy system on the ship. Moreover, paper [17] presents the results of parameter optimisation for this energetic system with particular interest in minimizing the capital costs, fuel costs, and CO₂ emissions. In turn, Shuli Wen et al. [18] presented an interval optimisation method for the same hybrid system. Among others, the authors came to the conclusion that the ship's rolling affected significantly the optimal efficiency of the energy storage system on the ship. A significant part of their research was applying a platform with six degrees of freedom to simulate the ship's swinging on the wave. The platform was lit with artificial light from xenon lamps. However, the heeling angles were limited to ±16°, and the

rolling period, characteristic of the tanker in question, was assumed as 20s.

Uncertainty due to the ship's motion on the wave, as well as the assumed ship's course and resulting fluctuations of power generated by PV panels, contribute significantly also to ageing of the storage which is an integral part of the ship's PV installation. It is also important to match the storage capacity to these changing conditions. The authors of paper [19] propose a binary system of energy storage, where some of the batteries are replaced by a super-capacitor, which allows the batteries to be changed less frequently. The paper presents a model of the ship's motion on the wave and a model of solar radiation on the ship in motion with PV panels, which allows the power of the hybrid PV system to be determined. The PV panels are of a universal character and can be used for other ships as well.

Technical-economic analysis of the hybrid PV system with application of super-capacitors only is, in turn, the subject of paper [20]. Analysis by applying single and multi-criteria evaluation methods was carried out on the example of the COSCO TENGFEI PCTC (car and truck carrier). The analysis proved that the application of the hybrid PV system has significant financial and environmental benefits.

In paper [21], a strategy is proposed to examine the impact of ship movements on the PV power system mounted on board. The proposed theoretical model makes it possible to determine the PV output power fluctuations according to the panels' tilt angle changes with respect to the sun.

The quoted papers usually concern some specific vessel, operated on a given route. Each designer's target is to create a power system for a new ship so that a solution with the highest possible efficiency is applied. Thus, any information concerning factors that distort the proper operation of the ship's power systems is crucial. When PV panels are used, it is important to know their power drop resulting from the ship's swinging on various courses in relation to the direction of solar radiation. Ships are characterised by diverse rolling periods as well as varied heeling angles, which, in turn results in changes of the power generated by PV panels.

The aim of the present paper is to determine the effect of the ship's rolling and incidence angle on the power generated by PV panels in real weather conditions, on the basis of experimental research.

SHIP'S MOTION ON THE WAVE

A ship's motion on the wave affects significantly the operation of a number of the appliances used on the ship. For this reason, some of them, such as handling machines, must be designed with attention to possible swinging of the ship which causes periodic tensions that lead to fatigue damage. In particular situations, for example during strong storms, excessive overload of mechanical devices can occur and threaten catastrophic damage [22, 23]. In the case of PV panels, because of their relatively small mass, the effect of the ship's swinging on the construction of the panels themselves,

as well as on the fastening devices, is negligible. Changes of the irradiance angles on the surface of the PV panels should be handled with more attention, however, because they affect the panels' efficiency.

The ship's swinging should be understood as oscillating linear and angular motions generated by the impact of the wave on the ship. In order to describe the ship's movement, e.g. in research on the swinging, two Cartesian coordinate systems are generally applied. One of them is the Earth-fixed O_0, x_0, y_0, z_0 system, where the x_0 and y_0 axes are in the plane of calm water, and the z_0 axis is directed vertically downwards. The second one is the G, x, y, z moving system and it is rigidly fixed on the ship. Its origin is located in the ship's centre of gravity G , the x, y axes are in the plane parallel to the structural waterline, whereby the x axis is directed towards the prow of the ship, the y axis towards the starboard, and the z axis vertically downwards [24]. It is assumed that the ship performs six types of oscillatory motion. They are progressive or rotary dislocations as related to the coordinate system fixed on the ship. Particular motions and their standard denotations are shown in Fig. 1, after paper [25].

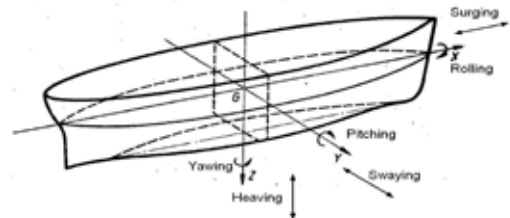


Fig. 1. Oscillatory motions of the ship

The dislocations are functions in time, as follows in Eqs. (1)-(6):

- surging (progressive displacements relative to axis x):

$$x(\tau) = X_A \sin(\omega\tau + \beta_x) \quad (1)$$

- swaying (progressive displacements relative to axis y):

$$y(\tau) = Y_A \sin(\omega\tau + \beta_y) \quad (2)$$

- heaving (progressive displacements relative to axis z):

$$z(\tau) = Z_A \sin(\omega\tau + \beta_z) \quad (3)$$

- rolling (rotational displacements relative to axis x):

$$\varphi(\tau) = \phi_A \sin(\omega\tau + \beta_f) \quad (4)$$

- pitching (rotational displacements relative to axis y):

$$\theta(\tau) = \Theta_A \sin(\omega\tau + \beta_t) \quad (5)$$

- yawing (rotational displacements relative to axis z):

$$\psi(\tau) = \Psi_A \sin(\omega\tau + \beta_p) \quad (6)$$

Big waves, which are particularly important for the ship's behaviour, are the so-called wind waves generated by the wind's effect on the free water surface. Big waves have wavelengths comparable with the main dimensions of the ship ($L \times B \times T$). By a strong wind, which is a random process, a storm wave is generated and it is very irregular (random), spatial, and characterised by profile asymmetry. When the wind stops blowing, or the wave reaches regions where there is no wind, it turns into a swell, approximating a regular wave.

If we assume that irregular waving is a stochastic process, homogeneous in space and stationary in time, then it can be presented as a double (relative to the frequency and direction of propagation), infinite sum of elementary harmonic waves with various frequencies and various directions of propagation. The above presentation of wave behaviour facilitates the meaningful determination of the statistical characteristics of the ship's swinging on irregular waves, if they are described by means of linear second order differential equations with constant coefficients [24]. The issue of waving has been discussed in a number of papers, i.a. [22-27]. They also give differential equations for the ship's swinging for both regular and irregular waves. The aim and necessities of this paper do not require further insight on this issue.

In many fields of shipbuilding, it is sufficient to consider only simple swinging, that is, one degree of freedom motion. Then, swinging occurs in the ship's symmetry plane (pitching), or in the plane of the cross-section of the hull (rolling). The attitude is justified because rolling, owing to its intensity, directly affects the ship's stability, and the safety and operational efficiency of some systems. That is why this motion is particularly significant [24]. However, when only simple rolling is considered, the other motions of the ship being neglected, the presentation of real conditions is quite coarse, although still acceptable in investigations on the effect of the swinging on the efficiency of the PV system.

RESEARCH STAND AND MEASUREMENT METHODOLOGY

The scheme of the working stand is presented in Fig. 2. The basic construction element of the stand was a movable platform (2) with a PV panel (1) and counterweight (6). The swinging motion of the platform with the PV panel was driven by an electric screw actuator (3) with adjustable velocities of sliding movement, which made it possible to obtain frequency changes of the platform's oscillation and thus simulate various rolling periods of a ship. The construction of the stand also enabled control of the rod stroke length, and so the amplitude (tilt) in the range of 0° to max. -25° and $+25^\circ$. The actuator was supplied by a power pack (4). A pyranometer with a CMP3 sensor was used to measure total irradiance. Data from the pyranometer (7) (irradiance) was registered in a data recorder (8) every 1s, as well as the electrical quantities (voltage and current) from the PV panel, which made it possible to determine its instantaneous electric power. The data were periodically transferred to a PC (5).

A PV panel of the type SV60M.2-300 from Selifa GE S.A. with power of 308.7 W was used in the research. The panel was tested earlier in industrial laboratory conditions and its parameters were precisely determined. The surface areas of the PV panel brutto and netto equalled respectively: $(0.992 \text{ m} \times 1.650 \text{ m}) 1.6368 \text{ m}^2$, and $(0.942 \text{ m} \times 1.6 \text{ m}) 1.5072 \text{ m}^2$. The load of the PV panel was 22Ω . The stand was placed on a trolley with rotary wheels in order to facilitate changes of the PV panel's position relative to the direction of solar radiation.

Experimental research was carried out in the first half of 2021 under a cloudless sky, on 22 and 25 February. The investigation was carried out in real conditions, and the research stand was located outside the university building. Due to practically the same weather conditions, the changes in the power of the PV panel were influenced only by changes in its position in relation to the sun due to the rolling of the platform. On each measurement day, several measurement series for various positions of the platform's rotation axis in relation to the direction of the solar rays were made. Measurements were made for the maximal swing angle of the platform with the PV panel equal to $\beta = \pm 25^\circ$. The rocking period was changed in the range of 15-24 s. For technical reasons, the time of each measurement series was limited and did not exceed 15 minutes.

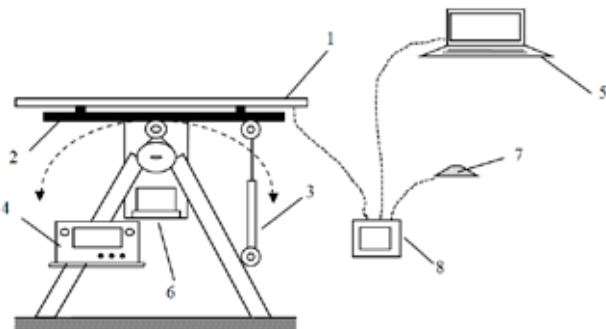


Fig. 2. Test stand for PV panels investigation (side view): 1 - PV panel, 2 - movable platform, 3 - electric screw actuator, 4 - actuator power pack, 5 - portable PC for the data processing, 6 - counterweight, 7 - pyranometer, 8 - recorder

Research was carried out for two variants of the position of the PV panel's rotation axis relative to the direction of solar radiation:

- variant A – the rotation axis of the platform with the PV panel was oriented perpendicularly to the direction of solar radiation,
- variant B – the rotation axis of the platform with the PV panel was oriented parallel to the projection of the direction of solar radiation on the plane of the PV panel.

DESCRIPTION OF VARIANTS OF RESEARCH ANALYSED

For the analysis, it was assumed that the stand simulated PV panels installed on a ship's deck, mounted in the horizontal plane with the panels' longer axes oriented parallel to the ship's axis of symmetry. A single PV panel was considered. Its position on the ship's deck is shown in Fig. 3. As a result of the action of waves, the ship with the PV panel was set in a rolling motion. As mentioned in the previous chapter, two extreme situations related to the orientation of the panel's rotation axis were investigated.

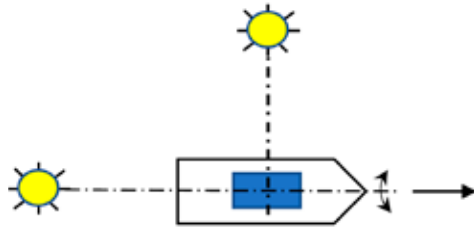


Fig. 3. Position of PV panel's rotation axis (ship's course) relative to direction of solar rays.

VARIANT A

Figures 4 and 5 present possible cases of the position of the PV panel's surface relative to the direction of solar radiation for variant A. It was assumed that a "minus" sign by angle denoted that the edge of the PV panel on the side of the direction of solar radiation was below its horizontal position, whereas a "plus" sign denoted that the edge of the PV panel was above the horizontal position. Fig. 4 presents four characteristic phases of the ship's roll in the case when the deck's surface with the PV panel moved in the direction of the Sun.

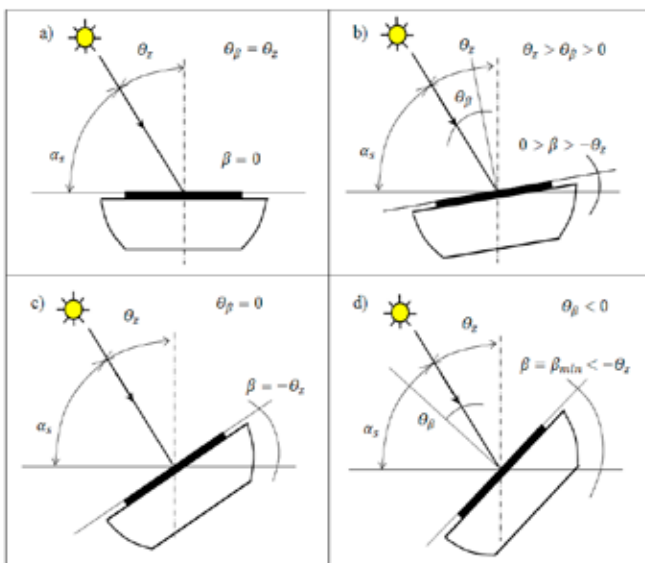


Fig. 4. Variant A – phases of ship's rolling when deck's surface with mounted PV panel moves in the direction of the sun

In turn, Fig. 5 shows four phases of the ship's roll when the ship moved in the direction opposite to the Sun. The incidence angle (Θ_β) depended on the current position of the Sun (α_s or Θ_z) and on the value of the inclination angle of the PV panel (β). The best position of the PV panel would be when the incidence angle Θ_β equalled zero (Fig. 4c). Motion of the PV panel from the zero position ($\beta = 0$) in the direction of the Sun caused a decrease of the value of the incidence angle Θ_β (Fig. 4a and 4b). If, in the maximal position, the value of the inclination angle of the PV panel $\beta = \beta_{min}$ is higher than the zenith angle Θ_z , then the panel's inclination angle values grow but they are negative.

Motion of the PV panel from the horizontal position ($\beta = 0$) in the opposite direction causes the value of the incidence angle Θ_β to increase (Fig. 5b) up to the value of 90° (Fig. 5c).

Further inclination of the PV panel up to the maximal position $\beta = \beta_{max}$ causes the value of the incidence angle Θ_β to be greater than 90° , which, in turn, causes the solar beams to strike the panel's back surface (Fig. 5d).

Thus, the PV panel's motion when its lower edge moves in the direction of the Sun causes the values of the incidence angles to be closer to their optimal values. As a result, the panel's power is higher than in the horizontal position. Motion of the PV panel in the opposite direction increases the values of the incidence angles in relation to the optimal value. The power of the PV panel achieved in the maximal position is then of the lowest value.

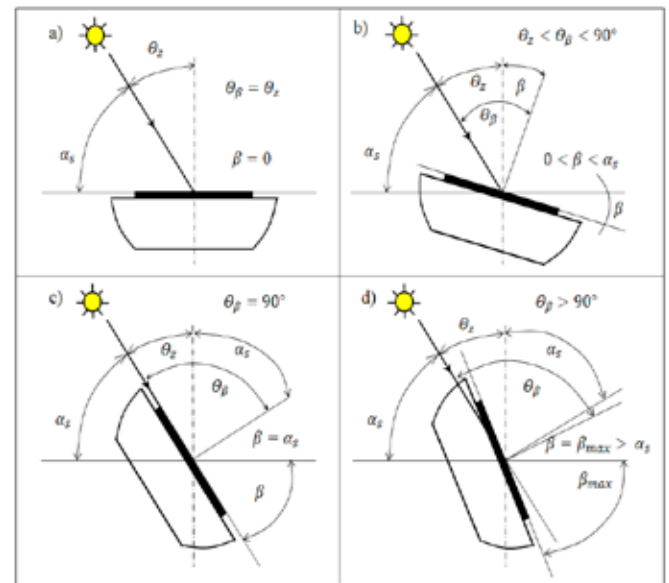


Fig. 5. Variant A – phases of ship's rolling when deck's surface with mounted PV panel moves opposite to the direction of the Sun

For variant A, the calculation methodology for the power generated by the PV panel is presented below.

A randomly chosen PV panel's rolling period was taken for consideration. The moment of maximal inclination of the PV panel in the direction from the Sun $\beta = \beta_{max}$ was assumed to be the beginning of the rolling period, and the moment the PV panel returned to the same position was assumed to end the rolling period. Dimensionless time, defined by dividing

a freely chosen time point in the period through the period's duration, was introduced in the analysis. Then, dimensionless times $\tau_r = 0$ and $\tau_r = 1$ referred to the beginning and the end of the rolling period. When $\tau_r = 0.5$, the PV panel was in the second maximal inclination, where its power was at its highest ($\beta = \beta_{min}$). In turn, for $\tau_r = 0.25$ and $\tau_r = 0.75$, the PV panel was in a horizontal position ($\beta = 0^\circ$). A fundamental problem was to determine how the rolling of the ship with the PV panel affected the change of power, as compared with the value of this parameter for the horizontal position of the PV panel. The relative power increment (increase or drop) of the PV panel was introduced into the analysis, considering 1m^2 of the panel's surface area, as defined by Eq. (7):

$$\Delta P_r(\tau_r) = \left[\frac{P_{\beta(\tau_r)} - P_{\beta=0^\circ}}{P_{\beta=0^\circ}} \right] / A_{PV} = \left[\frac{\Delta P(\tau_r)}{P_{\beta=0^\circ}} \right] / A_{PV} \quad (7)$$

If the shape of the equation describing the change of the above parameter in time is known, then it is possible to determine the amount of energy generated in one rolling period, by integrating this equation in the respective time periods.

The increase of the amount of energy generated by 1m^2 of the PV panel's surface while it is moving from the horizontal position ($\beta = 0^\circ$) to the position of its maximal inclination ($\beta = -25^\circ$) in the direction of the Sun and back to the horizontal position equals, according to Eq. (8),

$$\Delta E^+ = P_{\beta=0^\circ} \cdot \tau_c \cdot A_{PV} \cdot \int_{0.25}^{0.75} \Delta P(\tau_r) d\tau_r \quad (8)$$

The drop in the amount of energy generated by 1m^2 of the PV panel's surface while it is moving from the horizontal position (the inclination angle of the platform equals zero) to the position of its maximal inclination $\beta = +25^\circ$ in the direction opposite to the Sun equals, according to Eq. (9),

$$\Delta E^- = P_{\beta=0^\circ} \cdot \tau_c \cdot A_{PV} \cdot \left[\int_0^{0.25} P(\tau_r) d\tau_r + \int_{0.75}^1 P(\tau_r) d\tau_r \right] \quad (9)$$

Thus, the energy increment of the PV panel in the time period under analysis equals, according to Eq. (10),

$$\Delta E = \Delta E^+ + \Delta E^- \quad (10)$$

VARIANT B

Fig. 6 presents three characteristic positions of the PV panel for Variant B. The panel can incline in the clockwise direction, or the counterclockwise direction looking from the side of the solar radiation. The "minus" sign by angle β means inclination of the PV panel in the counterclockwise direction, and the "plus" sign means the panel's inclination in the clockwise direction looking from the side of the irradiance.

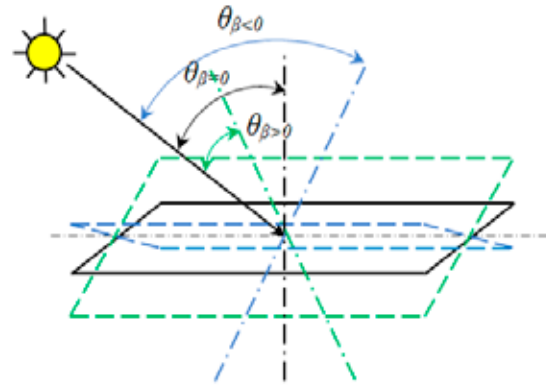


Fig. 6. Variant B – phases of ship's rolling when deck's surface moves clockwise and counterclockwise to the Sun looking from the side of solar radiation

The best position of the PV panel for this variant is the horizontal position. The incidence angle is then the closest to optimal. Left or right motion of the PV panel causes the value of the incidence angle to be higher than its value in the horizontal position of the PV panel. It should be noted that the values of the incidence angles in the maximal inclination of the panel are equal. The PV panel generates the highest power in the horizontal position and the lowest in the positions of maximal inclination.

The calculation methodology of the power changes, that is, of the amount of electric energy generated by the PV panel for variant B, is similar to that for variant A. The increment of the electric energy generated by the PV panel in the considered period can be calculated from relation (11):

$$\Delta E = 2 \cdot P_{\beta=0^\circ} \cdot \tau_c \cdot A_{PV} \int_0^{0.5} \Delta P(\tau_r) d\tau_r \quad (11)$$

RESEARCH RESULTS AND DISCUSSION

CALCULATIONS METHODOLOGY

The research results are presented in the form of diagrams only for the chosen research series, where the PV panel was moved by simulation of the ship's rolling. For each investigated case, the first of the diagrams shows the power changes of the PV panel and total irradiance on its surface as a function of time, respectively. On the basis of each first diagram, several regular and consecutive rolling periods were chosen. Then, the value of the average power of the PV panel in rolling conditions for these chosen periods was calculated. Depending on the start time of the analysed series, the PV panel's power was determined, in the horizontal position, before or subsequently to its rolling. Both power values were plotted in the diagram. In the next step, the difference between the instantaneous power of the PV panel and its power in the horizontal position was determined. Then, the relative power increment (increase or drop) of the PV panel

calculated per 1m² of the panel's surface was calculated from Eq. (7). This parameter can be written as a percentage. The analysis has been carried out for dimensionless time. So, the second of the analysed diagrams, shown below, presents percentage changes of the relative increase or drop in power calculated for 1m² of the PV panel's surface, in consecutive rolling periods.

COMPILATION OF THE TEST SERIES

Table 1 presents the characteristic data of the individual measurement series. The values given in the table: irradiance, power, power drop, and relative power drop, were averaged for the measurement time. The incidence angle was determined for the moment related to the mid-time of each series.

In turn, Table 2 shows the calculation results for the incidence angles on the PV panel's surface for the individual measurement series. Measurements were carried out for local Central European Time (winter time). Calculations were made for true solar time.

Table 2 presents also the values of the solar declination, solar azimuth, and the receiver's (PV panel) azimuth. The three last columns presented in Table 2 contain the calculation results of the incidence angles in the characteristic positions of the PV panel.

Tab. 1. Results of experimental research

Day/series/time	Var.	β	τ_c	\bar{G}	$\bar{P}_{\beta=0^\circ}$	$\bar{P}_{\beta(t)^\circ}$	$\Delta\bar{P}$	\bar{P}_r	$\theta_{\beta=0^\circ}$
		deg	s	W/m ²	W	W	W	1/m ²	deg
22.02.2021									
Series_1; 10:37 - 10:48	A	$\pm 25^\circ$	20	449.7	84.32	76.75	-7.57	-0.0596	67.4
Series_2; 11:02 - 11:10	B	$\pm 25^\circ$	20	467.9	87.99	87.39	-0.6	-0.0045	66.3
Series_3; 11:25 - 11:38	A	$\pm 25^\circ$	20	513.2	87.9	82.8	-5.1	-0.0385	65.1
25.02.2021									
Series_1; 9:33 - 9:41	A	$\pm 25^\circ$	15	219.0	77.13	63.54	-13.59	-0.1169	71.7
Series_2; 9:49 - 9:55	A	$\pm 25^\circ$	24	251.4	79.88	66.75	-13.13	-0.1091	70.3
Series_3; 10:04 - 10:10	A	$\pm 25^\circ$	18	323.7	81.41	70.53	-10.88	-0.0887	69.0
Series_4; 10:47 - 10:56	B	$\pm 25^\circ$	20	386.2	83.61	83.29	-1.32	-0.0105	65.7

Tab. 2. Calculation results for incidence angle

Day/series	Var.	δ	τ_{LT}	τ_{LST}	γ_s	γ	$\theta_{\beta=-25^\circ}$	$\theta_{\beta=0^\circ}$	$\theta_{\beta=+25^\circ}$
		deg	h:m	h:m	deg	deg	deg	deg	deg
22.02 /s1	A	-10.9	10:43	10:25	-25.4	-25.4	48.2	67.4	92.4
22.02 /s2	B	-10.9	11:06	10:49	-18.9	71.1	61.2	66.3	68.1
22.02 /s3	A	-10.9	11:30	11:15	-12.2	-12.2	41.5	65.1	90.0
25.02 /s1	A	-9.8	9:37	9:21	-41.8	-41.8	46.7	71.7	96.7
25.02 /s2	A	-9.8	9:52	9:35	-38.2	-38.2	45.4	70.3	95.4
25.02 /s3	A	-9.8	10:06	9:51	-34.6	-34.6	44.0	69.0	94.0
25.02 /s4	B	-9.8	10:51	10:35	-23.0	66.9	68.1	65.7	68.1

RESULTS AND DISCUSSION

Variant A

Fig. 7 shows a diagram of the stand's position in variant A. Prior to the measurements series, the setting of the research stand was amended and validated so that the assumed condition of perpendicularity of the platform's axis in relation to the direction of solar radiation could be maintained. In this position, the azimuth angle of the platform with the PV panel was equal to the solar azimuth angle.

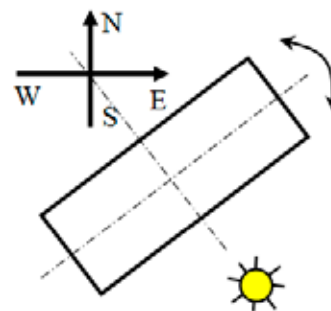


Fig. 7. Variant A: platform's axis of rotation positioned perpendicularly to direction of solar radiation

Figs. 8 and 9 present the research results for variant A carried out on 22 February 2021. In turn, Fig. 10 shows qualitatively the changes of the incidence angle when the platform with the PV panel was in three characteristic positions: one horizontal and two maximally tilted.

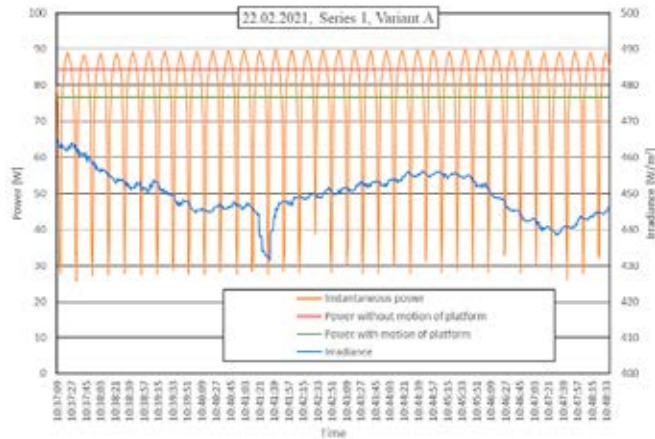


Fig. 8. Power and irradiance changes for variant A in research on 22 February 2021, $\tau_c = 20s$, series 1

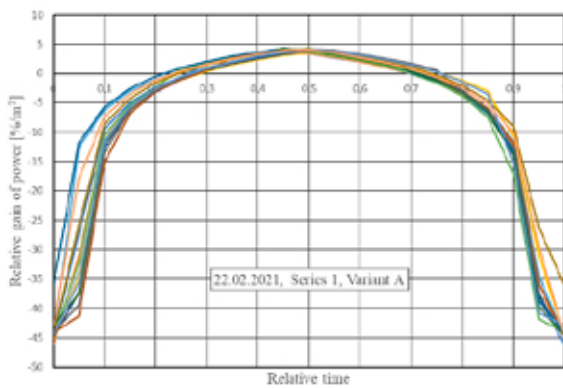


Fig. 9. Relative increase or drop of PV panel's power as a function of dimensionless time for variant A in research on 22 February 2021, $\tau_c = 20s$, series 1, several rolling periods

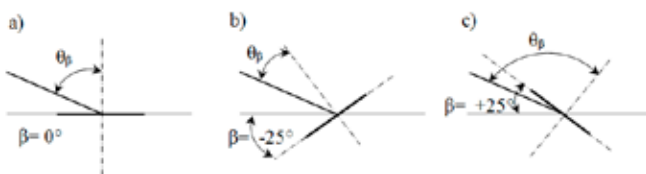


Fig. 10. Qualitative change of incidence angle θ_β depending on panel's inclination angle β

Fig. 8 shows power changes of the PV panel caused by the platform's motion and by instantaneous changes of irradiance that affect the value of generated power. Changes of the PV panel's power were of a regular character, related to the platform's rolling period. The panel reached the highest power values of ca 90 W with the platform's inclination in the direction of solar radiation, that is for $\beta = -25^\circ$, and the lowest power values of ca 30 W in the position opposite to the Sun, that is for $\beta = +25^\circ$. The above phenomenon resulted from the fact that the incidence angle to the PV panel was

$\theta_{\beta=-25^\circ} \approx 48.2^\circ$, and it was smaller from the angle $\theta_{\beta=0^\circ} \approx 67.4^\circ$ relative to the horizontal position of the PV panel (Figs. 10a and b, and Table 2). The least advantageous is the angle where the edge of the PV panel on the Sun side moves upwards ($\theta_{\beta=+25^\circ} \approx 92.4^\circ$ according to Table 2). During this motion, when the incidence angle was greater than 90° , the situation might occur where direct solar radiation did not meet the working surface of the PV panel, but only diffuse solar radiation and solar radiation reflected from objects neighbouring the research stand (Fig. 10c). This, in turn, caused the values related to the PV panel's lowest power to differ even by several Watts in consecutive periods. Fig. 8 shows two horizontal straight lines related to: the PV panel's mean power value during its motion (76.6 W) and the PV panel's mean power value when it remained in a horizontal position (84.3 W). In this case, the latter parameter was calculated as the mean power value of the horizontally positioned PV panel before and just after the calculation series. The mean value of total irradiance was 449.7 W/m^2 .

In turn, Fig. 9 shows the changes of the relative power increment of the PV panel per 1m^2 of its surface area as a function of dimensionless time for several chosen rolling periods. The time point when the PV panel's power was at its lowest value (i.e. for $\beta = +25^\circ$) was assumed to be the beginning and end of each of the analysed periods. Thus, for the maximally tilted PV panel, when $\beta = +25^\circ$ in the series under research, the relative drop of the instantaneous power of the PV panel could be lower than the value related to the horizontal position by as much as 45%. In the latter position, when $\beta = -25^\circ$, the relative increase of instantaneous power equalled only 5% of the power value at the horizontal position of the PV panel.

For variant A, also the effect of the rolling period on changes of the PV panel's characteristic parameters (Figs. 11-16) was investigated. The research was carried out on 25 February 2021, and the rolling periods were: 15s (series 1), 18s (series 3) and 24s (series 2), respectively. If the values of the obtained power values changed as a result of irradiance changes (Figs. 11, 13 and 15), then the runs illustrating the relative increase or drop of instantaneous power of the PV panel per 1m^2 of its surface area were similar in shape, regardless of the period (Figs. 12, 14 and 16).

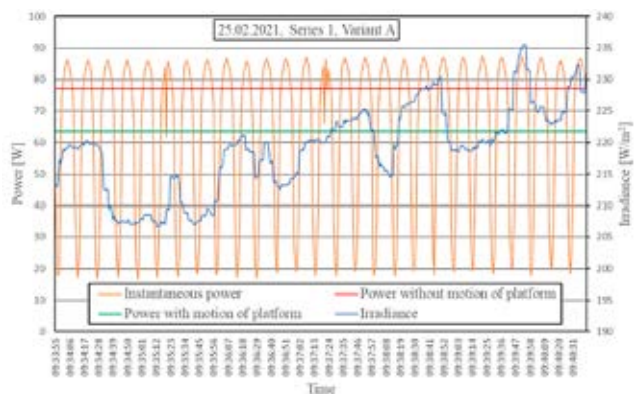


Fig. 11. Power and irradiance changes for variant A in research on 25 February 2021, $\tau_c = 15s$, series 1

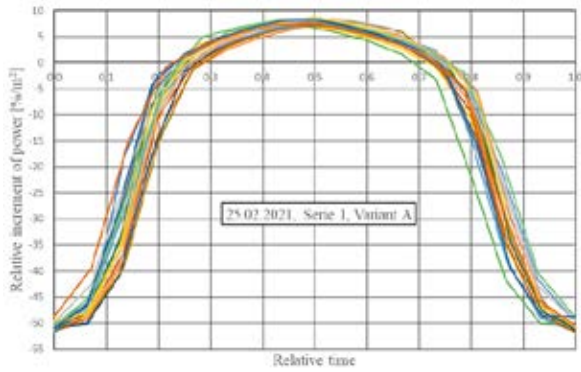


Fig. 12. Relative increase or drop of PV panel's power as a function of dimensionless time for variant A in research on 25 February 2021, $\tau_c = 15s$, series 1, several rolling period

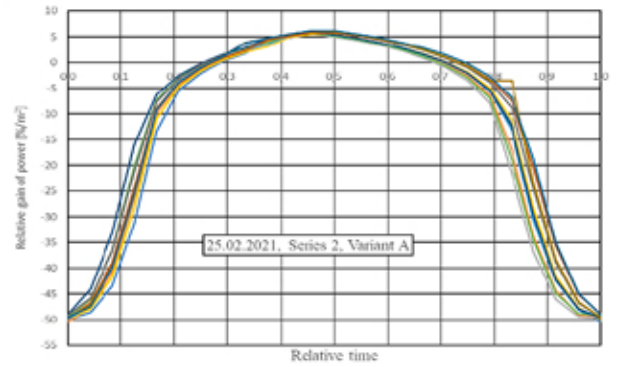


Fig. 16. Relative increase or drop of PV panel's power as a function of dimensionless time for variant A in research on 25 February 2021, $\tau_c = 24s$, series 2, several rolling periods

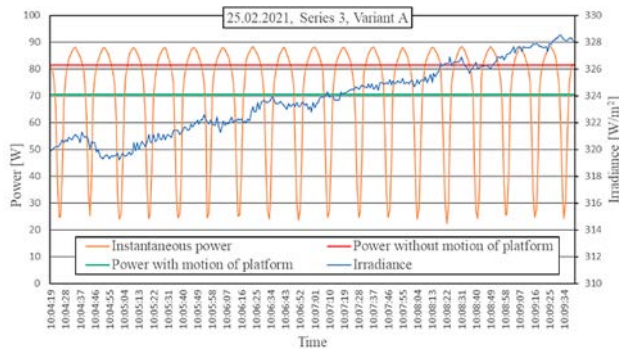


Fig. 13. Power and irradiance changes for variant A in research on 25 February 2021, $\tau_c = 18s$, series 3

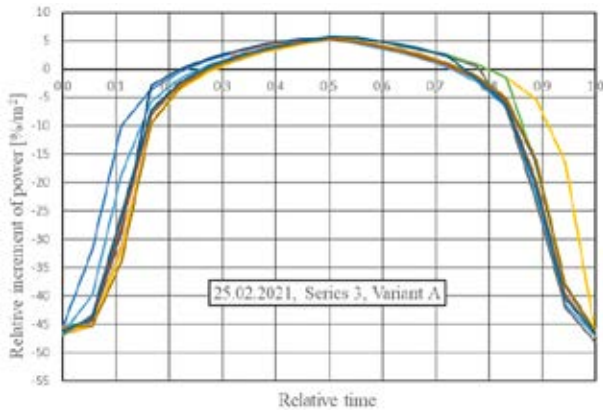


Fig. 14. Relative increase or drop of PV panel's power as a function of dimensionless time for variant A in research on 25 February 2021, $\tau_c = 18s$, series 3, several rolling periods

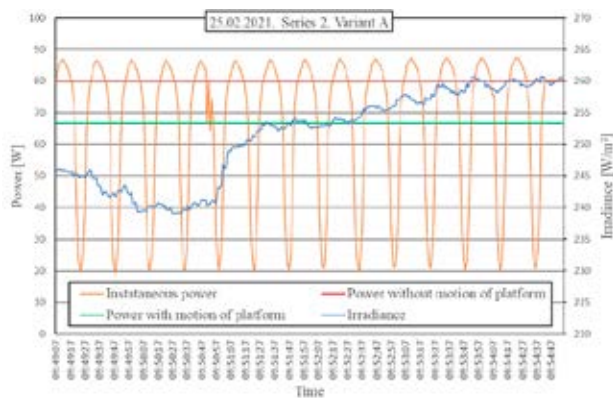


Fig. 15. Power and irradiance changes for variant A in research on 25 February 2021, $\tau_c = 24s$, series 2

Thus, the rolling period did not affect the obtained changes of the relative power increment ΔP ; however, a visible effect of the incidence angle θ_β could be observed. In the process of time, the incidence angle showed more advantageous values in all the characteristic positions of the PV panel. For the maximally tilted platform, that is for $\beta = +25^\circ$, the value of this angle gradually approached 90° , which caused more direct solar radiation to reach the exposed area of the PV panel. As shown in Figs. 12, 14 and 16, for the maximally tilted platform, the relative increment of instantaneous power of the PV panel was lower than the relative increment of instantaneous power of the PV panel in the horizontal position by ca 52%, 48% and 46%, respectively. A similar trend of changes of this parameter, but inverse, could be observed for the maximally tilted platform, when $\beta = -25^\circ$.

If the rolling period has no significant effect on changes of the relative power increment of the PV panel, then the research results for variant A shown in Table 1 can be presented as a relation of the relative power decrement $\Delta \bar{P}$, only for incidence angle θ_β , for the horizontal position of the PV panel (Figs. 17 and 18).

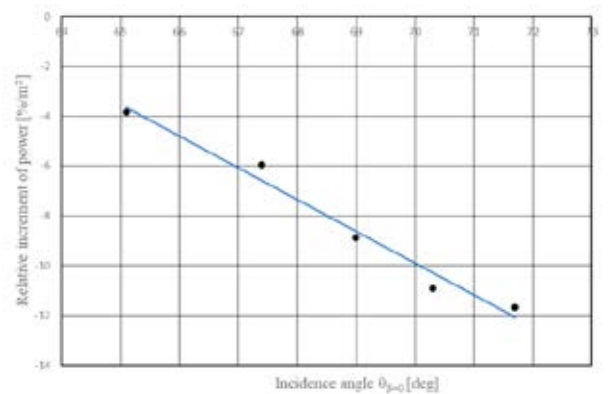


Fig. 17. Relative power decrement of PV panel as a function of incidence angle θ_β

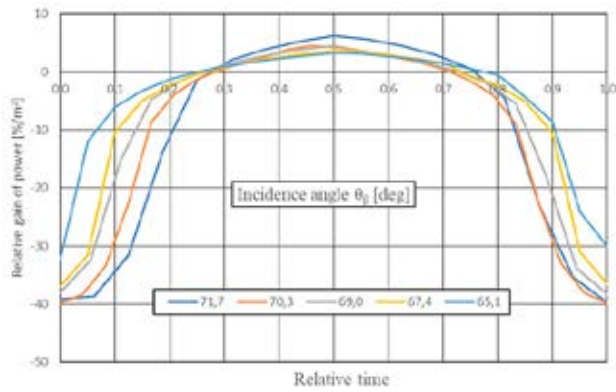


Fig. 18. Relative increase or drop of PV panel's power as a function of incidence angle θ_β and dimensionless time τ_r

Fig. 17 shows also the trend of changes for this parameter. It was stated for the range of changes of the parameter under research that the lower the value of incidence angle θ_β is, the smaller the absolute values of the relative power decrement ΔP_r of the PV panel, because the value of incidence angle θ_β is closer to its optimal value. This conclusion confirms the research results presented in Fig. 18. For smaller values of the incidence angle, runs illustrating the relative decrements of the PV panel's instantaneous power are flatter; that is, they gradually approach the straight line related to the value of this parameter obtained for the horizontal position.

VARIANT B

Fig. 19 illustrates the orientation of the rotation axis of the platform with the PV panel, relative to the direction of solar radiation. At the starting point of the measurements, the azimuth angle of the platform with the PV panel was 90° greater than the solar azimuth angle (the azimuth angle of the panel measured in relation to its shorter axis). Research with the platform in motion was carried out on 22 February (series 2) and 25 February 2021 (series 4) (Table 1).

The research results are presented in Figs. 20–24. The irradiance on 22 February was higher than on 25 February (Figs. 20 and 23). However, in both analysed series, the value of irradiance at the time of the research varied only minimally. As expected, the difference between the highest and the lowest values of instantaneous power of the PV panel was small and equalled only ca 1.0–1.5 W during one rolling period. The PV panel generated the best power in the horizontal position of the platform. On the other hand, with the platform tilted to the maximum, the values of the PV panel's power were found to be lower, but not always equal.

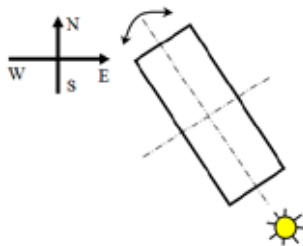


Fig. 19. Variant B; rotation axis of the platform parallel to direction of projection of solar radiation on the PV panel

As can be assumed, the asymmetry in power generation in both these positions of the platform in the initial phase of the series could be due to a slight inclination in the position of the rotation axis of the PV panel from the direction of solar radiation. Another reason for this asymmetry may be a lack of perfect levelling of the trolley with the platform, and as a result, minimal differences in the maximal tilt angles on both sides of the platform.

As the results presented in Fig. 20 show, in consecutive periods of the platform's motion, the changes in the instantaneous power of the PV panel in its maximally tilted positions become the same with time (symmetric).

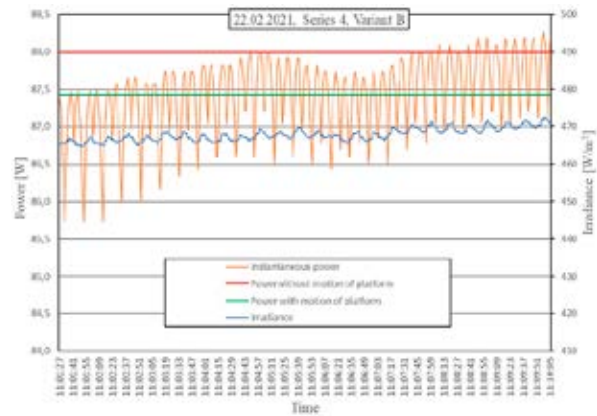


Fig. 20. Change of power and irradiance for variant B in research on 22 February 2021, $\tau_r = 20s$, series 2

The above trend of power changes was, however, not observed for the series of research carried out on 25 February 2021 (Fig. 23). The lack of the symmetry could be caused by different values of solar radiation reflected from objects that surrounded the research stand, or from various albedo values of the ground in situations when the platform is maximally tilted. Figs. 21–22 show changes of the relative increment of power as a function of the dimensionless time for the first and the last rolling period of the PV panel on 22 February 2021. The PV panel's power in the horizontal position, with the motionless platform, and before the start of the first rolling period, was 87.39 W, and its mean power in the rolling period was 86.93 W. The mean values of the above parameters during inclinations in the time analysed differed only slightly. So, it is difficult to quantitatively estimate the research results obtained. Their analysis can only be of a qualitative character. In this research series, the mean irradiance equalled 465.6 W/m^2 . The difficulty in quantitative estimation of the research results occurs also for the last of the rolling periods. After the end of the last period, the PV panel's power was 88.44 W, and its mean power during the platform's motion was 87.78 W. For the maximally tilted platform, the values of the relative instantaneous powers of the PV panel were nearly the same. Hence, it could be claimed that, for this period, the rotation axis was ideally parallel to the direction of solar radiation and the trolley was perfectly levelled. The value of mean irradiance for this period was ca 470.9 W/m^2 .

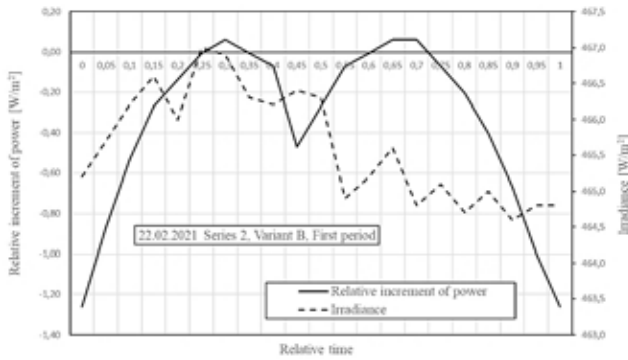


Fig. 21. Relative increment of PV panel's power as a function of dimensionless time for variant B in research on 22 February 2021, $\tau_c = 20s$, series 2; first period

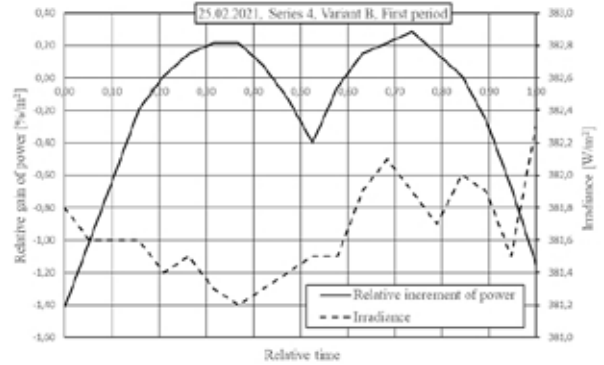


Fig. 24. Relative increment of PV panel's power as a function of dimensionless time for variant B in research on 25 February 2021, $\tau_c = 20s$, series 4, first period

The trend of changes of the relative increment of instantaneous power as shown in Fig. 21 can be observed also by analysis of the research results shown in Fig. 24, for the first period of the research series carried out on 25 February 2021.

CONCLUSIONS

By contrast with conditions onshore, exact estimation of the performance of a PV system mounted on a ship is difficult because of the ship's motions on the waves, as well as of changes in time of the geographical coordinates of the ship's position in relation to the Sun. The most serious disturbance is the ship's rolling, characterised by the highest amplitude of inclinations. That is why the range of research has been limited to the above case. Detailed analysis was applied to two characteristic positions of the rotation axis of the PV panel, that is, perpendicular to the direction of solar radiation (variant A), and parallel to the solar radiation's projection on the horizontal plane (variant B). The possible loss of electrical energy by the PV panels due to rolling was determined. On the basis of the analysis of the research results and theoretical considerations, the following general and detailed conclusions are determined.

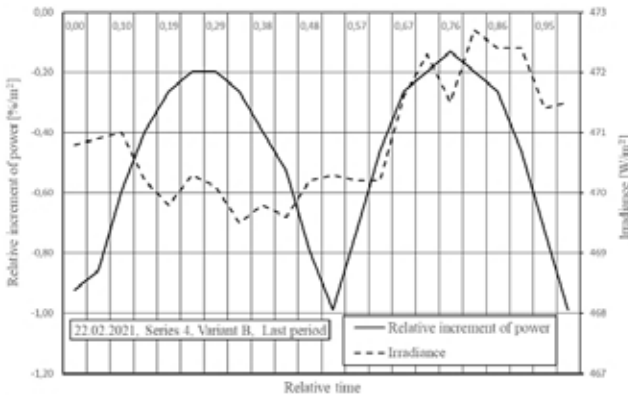


Fig. 22. Relative increment of PV panel's power as a function of dimensionless time for variant B in research on 22 February 2021, $\tau_c = 20s$, series 2; last period



Fig. 23. Change of power and irradiance for variant B in research on 25 February 2021, $\tau_c = 20s$, series 4

General conclusions:

- the instantaneous power generated by the PV panel changes periodically with a frequency equal to the frequency of the ship's rolling,
- the mean power generated by the PV panel during the ship's rolling is less than the power generated by the PV panel in a horizontal position,
- most of all, the mutual relation between the inclination angle of the PV module and the incidence angle is decisive for the drop of power generated by the PV panel,
- the effect of rolling on the PV panel's power can be estimated by means of the relative power increment generated from $1m^2$ of its surface area.

Detailed conclusions:

Variant A

- in the range of changes under research, the highest power values were achieved by the PV panel when the platform was inclined in the direction of solar radiation, and the lowest values in the position opposite to the direction of solar

- radiation; the reasons are the more or less advantageous incidence angles on the exposed surface,
- b) at a small solar elevation and respectively a big ship's tilt, the incidence angle can be more than 90°, as a result of which solar rays contact the back surface of the PV panel, causing a drop in its power which depends, in this position, only on the solar radiation dispersed and reflected from neighbouring objects next to the research stand,
 - c) changes of the relative increment of the PV panel's power per 1m² of its surface area in the dimensionless time function have similar shapes, regardless of the rolling period,
 - d) changes of the relative power increment of the PV panel in the time function can be approximated by a polynomial, and the best fitting was obtained for a fourth degree polynomial,
 - e) the rolling period does not significantly affect the increment of relative power,
 - f) in the range of parameter changes under research, the relative drops of power increments of the PV panel increase with expansion of the incidence angle on the horizontal surface of the PV panel.

Variant B

- a) the highest power value was generated by the PV panel in the horizontal position of the platform,
- b) for a maximally tilted platform, the power values of the PV panel were slightly lower, but not always the same because of a probable small inclination of the rotation axis of the PV panel from the direction parallel to the projection of solar radiation,
- c) the lack of symmetry of the power values for opposite positions of the maximally tilted platform may be caused by different values of solar radiation reflected from neighbouring objects next to the research stand, by different albedo of the ground, a slight inclination in the position of the rotation axis of the PV panel from the direction of solar radiation, or a lack of perfect levelling of the trolley with platform.

The authors will presently elaborate the research results for intermediate positions of the platform's axis relative to the direction of solar radiation.

ACKNOWLEDGEMENT

The authors thank sincerely the Selfa GE S.A. company in Szczecin for providing the PV panels for this research.

REFERENCES

1. International Maritime Organization, (2022) 'Initial IMO GHG Strategy' [Online]. Available: <https://www.imo.org/en/MediaCentre/HotTopics/Pages/Reducing-greenhouse-gas-emissions-from-ships.aspx>.
2. W. Tarelko, 'The effect of hull biofouling on parameters characterizing ship propulsion system efficiency', *Polish Maritime Research*, No. 4 (85), Vol. 21; pp. 27-34, 2014, DOI:102478/pmr-2014-0038.
3. C. Dymarski, 'A concept design of diesel-hydraulic propulsion system for passenger ship intended for inland shallow water navigation', *Polish Maritime Research*, No. 3 (103), Vol. 26; pp. 30-38, 2019, DOI:102478/pmr-2019-0043.
4. W. Litwin, D. Piątek, W. Lesniewski, K. Marszałkowski, '50' Sail catamaran with hybrid propulsion, design, theoretical and experimental studies', *Polish Maritime Research*, No. 2 (114), Vol. 29; pp. 12-18, 2022, DOI:102478/pmr-2022-0012.
5. M. Kunicka, W. Litwin, 'Energy efficient small inland passenger shuttle ferry with hybrid propulsion-concept design, calculations and model tests', *Polish Maritime Research*, No. 2 (102), Vol. 26; pp. 85-92, 2019, DOI:102478/pmr-2019-0028.
6. P. Geng, 'State of charge estimation method for lithium-ion batteries in all-electric ships based on LSTM neural network', *Polish Maritime Research*, No. 3 (107), Vol. 27; pp. 100-108, 2020, DOI:102478/pmr-2020-0051.
7. J. Lv, Y. Lin, R. Zhang, B. Li and H. Yang, 'Assisted propulsion device of a semi-submersible ship based on the Magnus effect', *Polish Maritime Research*, No. 3 (115), Vol. 29; pp. 21-34, 2022, DOI:102478/pmr-2022-0023.
8. O. Konur and K. E. Erginer, 'Effect of sea water cooling systems to the energy efficiency of solar panels on marine vessels' in *Proceedings of the 2nd Global Conf. on Innovation in Marine Technology and Future of Marine Transportation, Bodrum, Mugla, Turkey, 2016*.
9. O. Konur, S. A. Kormaz, O. Yuksel, Y. Gulmez, A. Erdogan, K. E. Erginer, C. O. Colpan, 'Thermodynamic modelling of seawater cooled foldable PV panel system', in *Proceedings of the 7th Global Conf. on Global Warming (GCGW-2018), Izmir, Turkey, 2018*.
10. S. Odeh and M. Behnia, 'Improving photovoltaic module efficiency using water cooling', *Heat Transf. Eng.*, vol. 30, no. 6, pp. 499-505, 2009, doi:org/10.1080/01457630802529214.
11. K. A. Moharram, M. S. Abd-Elhady, H. A. Kandil, H. El-Sherif, 'Enhancing the performance of photovoltaic panels by water cooling', *Ain Shams Eng. J.*, vol. 4, no. 4, pp. 869-877, Dec. 2013, doi:org/10.1016/j.asej.2013.03.005.
12. M. K. Smith, H. Selbak, C. C. Wamser, N. U. Day, M. Krieske, D. J. Sailor, T. N. Rosenstiel, 'Water cooling method to improve the performance of field-mounted, insulated, and concentrating photovoltaic modules', *ASME J. Sol. Energy Eng.*, vol. 136, no. 3, Aug. 2014, doi:org/10.1115/1.4026466.

13. Z. Zapałowicz and W. Zeńczak, 'The possibilities to improve ship's energy efficiency through the application of PV installation including cooled modules', *Renew. Sustain. Energy Rev.*, vol. 143, pp. 1-16, 2021, doi:org/10.1016/j.rser.2021.110964.
14. I. Kobougias, E. Tatakis, J. Prousalidis, 'PV systems installed in marine vessels: technologies and specifications', *Adv. Power El.*, vol. 2013, pp. 1-8, doi:org/ 10.1155/2013/831560.
15. W. Laursen, 'Putting solar technology into the hybrid mix', *Motor Ship*, vol.. 3, pp. 24-27, Apr. 2012.
16. L. Hai, B. Yifei, W. Shuli, C. Y. David, H. Ying-Yi, D. Jinfeng, P. Cheng, 'Modeling and stability analysis of hybrid PV/diesel/ESS in ship power system', *Inventions*, vol. 1, no. 1, 2016, doi: org/10.3390/inventions1010005.
17. H. Lan, S. Wen, Y. Y Hong , D. C. Yu, L. Zhang, 'Optimal sizing of hybrid PV/diesel/battery in ship power system', *Appl. Energy*, vol. 158, pp. 26-34, Nov. 2015, doi:org/10.1016/j.apenergy.2015.08.031.
18. S. Wen, H. Lan, Y. Y. Hong, D. C. Yu, L. Zhang L, P. Cheng, 'Allocation of ESS by interval optimization method considering impact of ship swinging on hybrid PV/diesel ship power system', *Appl. Energy*, vol. 175, pp. 158-167, 2016, doi:org/10.1016/j.apenergy.2016.05.003.
19. K. Liu, Q. Zhang, X. Qi, Y. Han, F. Lu, 'Estimation of PV output power in moving and rocking hybrid energy marine ships', *Appl. Energy*, vol. 204, pp. 362-372, 2017, doi:org/10.1016/j.apenergy.2017.07.014.
20. Y. Qiu, C. Yuan, J. Tang, X. Tang, 'Techno-economic analysis of PV systems integrated into ship power grid: A case study', *En. Convers. Manag.*, vol. 198, pp. 1-12, Aug. 2019, doi:org/10.1016/j.enconman.2019.111925.
21. S. Nasiri, M. Parniani, F. Blaabjerg, S. Peyghami, 'Analysis of all-electric ship motions impact on PV system output power in waves', in *Proceedings of 2022 IEEE/AIAA Transportation Electrification Conference an Electric Aircraft Technologies Symposium*, pp. 450-45, 2022, doi:10.1109/ITEC53557.2022.9813953.
22. M. Hann, 'Computer analysis of the reliability and safety of machinery and ship structures subjected to rocking' Gdańsk: Okrętownictwo i Żegluga, 2001.
23. K. Niklas, A. Karczewski, 'Determination of seakeeping performance for a case study vessel by the strip theory method', *Polish Maritime Research*, No. 4 (108), Vol. 27; pp. 4-16, 2020, DOI:102478/pmr-2020-0061.
24. J. Dudziak, 'Ship theory', Gdańsk: Fundacja Promocji Przemysłu okrętowego i Gospodarki Morskiej, 2008.
25. J. Dudziak, 'Ship on the wave', Gdańsk: Wydawnictwo Morskie, 1980.
26. M. K. Ochi, *Ocean Waves. The Stochastic Approach*, Cambridge: Cambridge University Press, 1998.
27. T. Szelangiewicz, 'Fundamentals of the theory of designing anchor systems for holding the position of vessels', Gdańsk: Okrętownictwo i Żegluga, 2003.

CONTACT WITH THE AUTHORS

Wojciech Zeńczak

e-mail: wojciech.zenczak@zut.edu.pl

Zbigniew Zapałowicz

West Pomeranian University of Technology
Szczecin
POLAND